

Contrasting provenance budgets for suspended load and bedload of the Yarlung Tsangpo, Tibet: Lhasa block or Himalaya?

Wendong Liang¹, Xiumian Hu^{2,*}, Eduardo Garzanti³, Xiaolong Dong², and Fengting Chen²

¹State Key Laboratory of Oil and Gas Reservoir Geology and Exploitation, Institute of Sedimentary Geology, Chengdu University of Technology, 610059 Chengdu, China

²State Key Laboratory for Mineral Deposits Research, School of Earth Sciences and Engineering, Nanjing University, 210023 Nanjing, China

³Laboratory for Provenance Studies, Department of Earth and Environmental Sciences, University of Milano–Bicocca, 20126 Milano, Italy

ABSTRACT

Sediments from the same river are typically thought to reflect a common provenance, even though they may record notably different, and even opposite, sediment supply and erosion signals. Such discrepancies can introduce significant bias into our interpretation of geomorphological processes. This study focuses on the Yarlung Tsangpo, the Tibetan headwaters of the Brahmaputra River, and contrasts mineralogical and geochemical information on suspended load in transit and on fluvial bars to reveal a major discrepancy in sediment budgets calculated with petrographic and isotopic data for sand and mud fractions. Our results show that in both suspended load and fluvial bars, sand records an overwhelming contribution from the Lhasa block, whereas mud reflects dominant supply from the Himalayan belt. Detritus from the Lhasa block is twice as abundant as Himalayan detritus in sandbars, but the Himalayan contribution is 1.4 times that of the Lhasa block in suspended load. Overall, Himalayan sedimentary rocks are estimated to generate as much sediment as Lhasa granitoid and volcanic rocks. Himalayan erosion rates and sediment yields are greatly underestimated if only sand, representing a subordinate part of the total sediment flux, is considered in sediment-budget calculations. Both sand-rich bedload and mud-rich suspended load must be given full consideration in the study of sediment-generation processes. Our results highlight the potential pitfalls of relying solely on sand-sized sediment in provenance analysis and force a reevaluation of how sediment yields and erosion patterns are assessed.

INTRODUCTION

Rivers are the primary sculptors of terrestrial landscapes and serve as vital conduits for the transport of weathered materials from the continental surface to the ocean (Allen, 2008). Accurately quantifying the sediment yield from different geological domains is the key to a correct reconstruction of geomorphological processes through geological history (Leeder, 2011; Resentini et al., 2017). Although the increasing integration of diverse analytical methods has significantly enhanced the precision of provenance analysis (e.g., von Eynatten et al., 2012, 2016; Garzanti et al., 2024), neglecting the compositional differences among different grain-size fractions can lead to substantial error in the assessment of provenance and erosion patterns.

Fluvial bars and suspended load are widely assumed to reflect the same provenance (e.g., Singh and France-Lanord, 2002; Jian et al., 2020; Stutenbecker, et al., 2023). However, there is a serious risk of misinterpreting sediment yields and erosion rates in river basins where source-rock lithologies exhibit markedly contrasting capabilities to generate sediment of different grain size (Garçon and Chauvel, 2014; Garzanti et al., 2021; Liedel et al., 2024).

Here we focus on the Yarlung Tsangpo, the Tibetan headwaters of the Brahmaputra River, which is characterized by rather homogeneous climatic and tectonic conditions on both sides of its course, whereas sharply contrasting rock assemblages are exposed to the north (largely magmatic rocks) and to the south (mostly sedimentary rocks) (Fig. 1). Previous studies based on sandbars suggested that Yarlung Tsangpo sediments were supplied mainly by the Lhasa block, with contributions from the Himalayan belt either


(1) overlooked based on geochemical analyses (Li et al., 2009; Wu et al., 2012), or (2) considered as subordinate based on the U-Pb age distribution of detrital zircon (Zhang et al., 2012; Ma et al., 2023) and apatite (Du et al., 2024) or on sand petrography and mineralogy (Liang et al., 2022). These studies, however, focused on the sand fraction only and may have thus significantly underestimated the capacity for mud production of Himalayan sedimentary rocks. The aim of this study is to reassess the sediment fluxes in southern Tibet and to show how the underestimation of differences in sand- and mud-generation potential between igneous and sedimentary rocks has led to misinterpretation of geomorphological processes and erosion patterns in this imposing orogenic setting.

GEOLOGICAL FRAMEWORK

The Yarlung Tsangpo catchment includes three main tectonic domains: the Lhasa block to the north, the intervening Indus-Yarlung suture zone, and the northern side of the Himalayan belt to the south (Fig. 1B). The Lhasa block consists mainly of the Gangdese arc batholith, Jurassic to Eocene volcanic rocks, and limited Paleozoic metasedimentary basement, with Mesozoic strata exposed in the north (Zhu et al., 2011). The Indus-Yarlung suture zone comprises Cretaceous to Eocene forearc-basin sediments along with their discontinuous ophiolitic basement and serpentinite-matrix mélange (Hu et al., 2015). The northern side of the Himalayan belt includes the Paleozoic to Eocene carbonate and siliciclastic succession of the Tethys Himalaya (Sciunnach and Garzanti, 2012), lower Paleozoic orthogneisses, and Miocene leucogranites (Carosi et al., 2019).

METHODS

Nine samples collected from active sandbars in November 2019 and 13 samples of suspended

Xiumian Hu  <https://orcid.org/0000-0002-5401-8682>
*huxm@nju.edu.cn

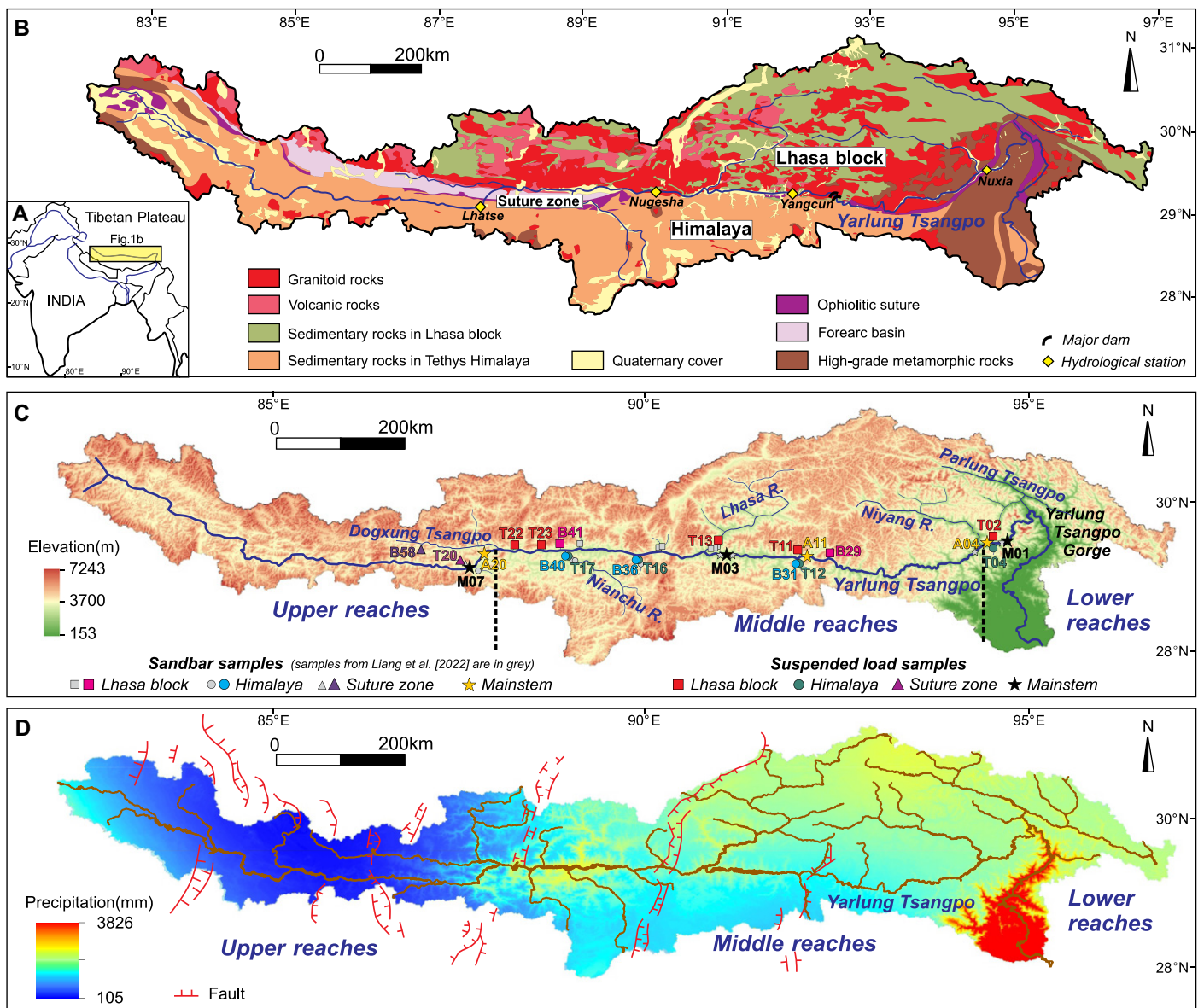


Figure 1. Yarlung Tsangpo catchment, Tibet. (A) Geographic location. (B) Geological map (modified after Pan et al., 2004). (C) Topography and sampling sites. (D) Precipitation (averaged values in July–August from 2012 to 2021; after Peng, 2024); southern Tibetan graben system is also shown.

sediment collected at the channel's midpoint during June–July 2023 were sieved to separate sand (63–2000 μm) and mud (<63 μm) fractions. The petrographic composition of the sand fraction in one sandbar and nine suspended-load samples was determined using the Gazzi-Dickinson method (Ingersoll et al., 1984). The strontium (Sr) and neodymium (Nd) isotopic signatures associated with trace elements were determined on the mud fraction of 12 suspended-load and nine sandbar samples. Sampling strategy, analytical procedures, and results are illustrated in the Supplemental Material¹.

¹Supplemental Material. Supporting analytical methods, figures, and data provided in this study. Please visit <https://doi.org/10.1130/GEOL.S.28250798> to access the supplemental material; contact editing@geosociety.org with any questions.

RESULTS

Petrography of the Sand Fraction

The sand fraction carried in suspension is feldspatho-litho-quartzose with minor sedimentary, volcanic, and metamorphic lithics in the Yarlung Tsangpo, ranges from quartzo-lithic to feldspatho-quartzo-lithic with shale, slate, siltstone, and metasandstone lithics in Himalayan tributaries, is litho-feldspatho-quartzose with plagioclase \geq K-feldspar in tributaries draining the Lhasa block, and is quartzo-lithic with abundant serpentinite, shale, slate, and sandstone lithics in streams draining the suture zone (Fig. 2).

In tributaries draining the Himalaya and the suture zone, the sand fraction has similar composition in suspended load and sandbars (Liang et al., 2022). Instead, in the Yarlung Tsangpo mainstem and in Lhasa block tributaries, the sand fraction is enriched in quartz and mica in

suspended load and in feldspar and metamorphic lithics in sandbars (Fig. 2).

Isotopic Signatures of the Mud Fraction

The $^{87}\text{Sr}/^{86}\text{Sr}$ ratio in the studied mud fraction appears to be independent of both sample grain size and longitude (used here as a proxy for rainfall and hence weathering intensity; Fig. S1 in the Supplemental Material). The strong correlation observed between $^{87}\text{Sr}/^{86}\text{Sr}$ and ϵNd ($R^2 = 0.80$, $P < 0.001$; Fig. 3A) thus indicates that source-rock lithology represents the primary control.

In the Yarlung Tsangpo, ϵNd values vary from -11.7 to -8.1 and $^{87}\text{Sr}/^{86}\text{Sr}$ from 0.712994 to 0.714293 in the mud fraction of suspended load, and ϵNd values vary from -12.0 to -7.5 and $^{87}\text{Sr}/^{86}\text{Sr}$ from 0.712029 to 0.715961 in the mud fraction of sandbars.

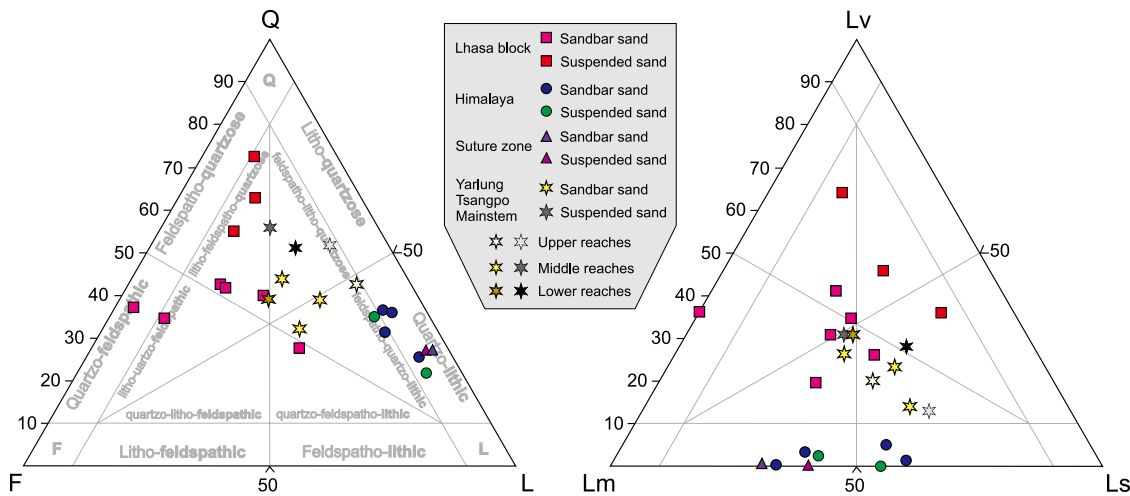


Figure 2. Sand petrography. Petrographic data of sandbars are from Liang et al. (2022). Compositional fields in QFL (Q—quartz; F—feldspar; L—lithic grains) diagram after Garzanti (2019). Lv—volcanic lithics; Lm—metamorphic lithics; Ls—sedimentary lithics.

Sediment carried by Himalayan tributaries is largely recycled from sedimentary rocks originally derived from old continental crust, which explains their higher $^{87}\text{Sr}/^{86}\text{Sr}$ (suspended load: 0.713558–0.718033; bars: 0.716457–0.718003) and negative ϵNd values (suspended load: -11.3 to -8.2 ; bars: -11.1 to -8.8). In contrast, Lhasa block tributaries draining subduction-related Gangdese granitoids and volcanic rocks are characterized by lower $^{87}\text{Sr}/^{86}\text{Sr}$ (suspended load: 0.708745–0.711760; bars: 0.706627–0.706657) and less-negative ϵNd (suspended load: -8.1 to -2.2 ; bars: -2.4 to -1.3) (Fig. 3). The mud fraction in the shorter northern tributaries draining only Lhasa block igneous rocks displays the lowest $^{87}\text{Sr}/^{86}\text{Sr}$ and the least-negative ϵNd values relative to that in the tributaries (represented by sample T13 and T02; Fig. 3A) also draining Mesozoic sedimentary rocks and Paleozoic and Precambrian metasedimentary rocks exposed in the central and northern Lhasa block (Fig. 1). The mud fraction in one tributary draining only the ophiolitic suture zone shows similar isotopic ratios as Himalayan tributaries (suspended

load: $\epsilon\text{Nd} -10.1$ and $^{87}\text{Sr}/^{86}\text{Sr} 0.716084$; bar: $\epsilon\text{Nd} -10.9$ and $^{87}\text{Sr}/^{86}\text{Sr} 0.713839$) (Fig. 3A).

Provenance Budgets

Forward mixing calculations indicate that the sand fraction of Yarlung Tsangpo suspended load is derived mostly from the Lhasa block ($85\% \pm 4\%$ in middle reaches and $80\% \pm 8\%$ in lower reaches), with lesser contributions from the Himalayan belt ($8\% \pm 5\%$ and $15\% \pm 8\%$, respectively) and suture zone ($8\% \pm 3\%$ and $5\% \pm 0\%$, respectively) (Fig. 4). Similar percentages were estimated for the sand fraction in Yarlung Tsangpo sandbars, dominated by supply from the Lhasa block ($71\% \pm 11\%$ in middle reaches and $78\% \pm 12\%$ in lower reaches), with subordinate contribution from the Himalayan belt ($24\% \pm 10\%$ and $14\% \pm 9\%$, respectively) and suture zone ($5\% \pm 3\%$ and $8\% \pm 7\%$, respectively; Liang et al., 2022) (Fig. 4).

The Sr and Nd isotopic signatures of suture-zone and Himalayan sources are indistinguishable (Fig. 3), but trace elements such as Cr and Ni clearly differentiate them. Based on key trace elements, the suture zone's contribution can be

reliably assessed to be minimal for suspended mud from upper ($5\% \pm 4\%$) to lower reaches ($3\% \pm 3\%$) of the Yarlung Tsangpo and negligible for sandbar mud in all reaches ($\sim 0\%$). The source of the mud fraction can thus be safely constrained by considering as end members the observed Sr and Nd isotopic signatures of the Himalayan belt and Lhasa block only. Mixing calculations indicate that Yarlung Tsangpo mud is derived mostly from the Himalayan belt in both suspended load ($62\% \pm 19\%$ in middle reaches and $78\% \pm 16\%$ in lower reaches; Figs. 3C and 4) and sandbars ($71\% \pm 4\%$ and $75\% \pm 3\%$, respectively) (Figs. 3B and 4).

DISCUSSION

The Grain-Size Factor: Mud versus Sand

In the Yarlung Tsangpo, consistent provenance indications are obtained for mud and sand fractions whether they belong to suspended load or sandbars (Fig. 4). In contrast, suspended-load mud and bedload sand convey opposite provenance indications: the Lhasa block is calculated to contribute five times more sand than the Himalayan belt, and the Himalayan belt between two

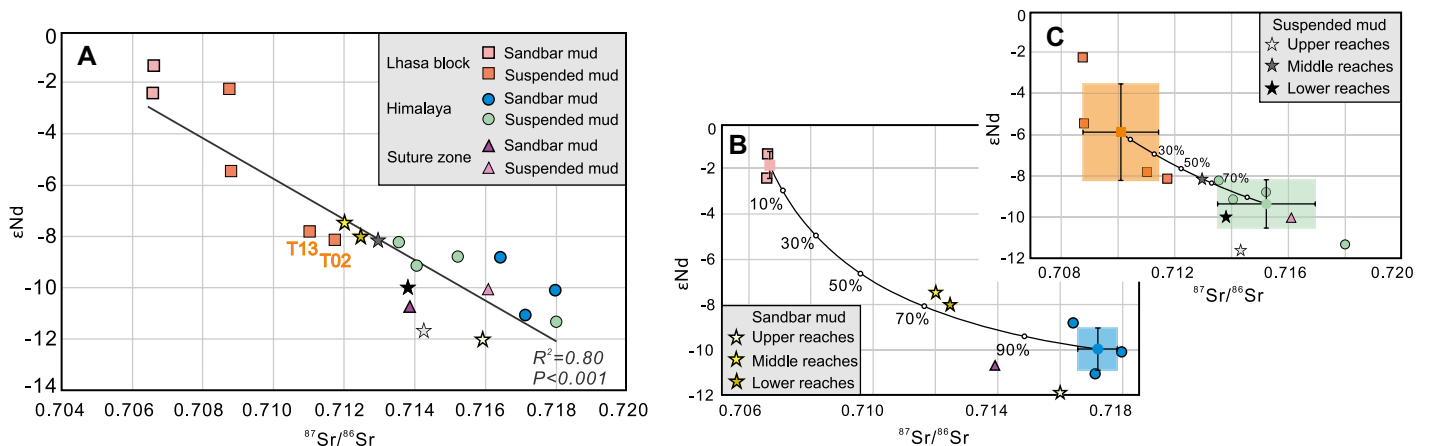


Figure 3. Sr-Nd isotopic ratios for mud fraction (A), and binary mixing model showing relative contributions from Himalayan belt and Lhasa block to mud in sandbars (B) and suspended load (C). T02 and T13 are suspended load samples indicated in Fig. 1C. The colored boxes represent mean isotopic values with ± 1 standard deviation. See Figure 1 for locations of reaches.

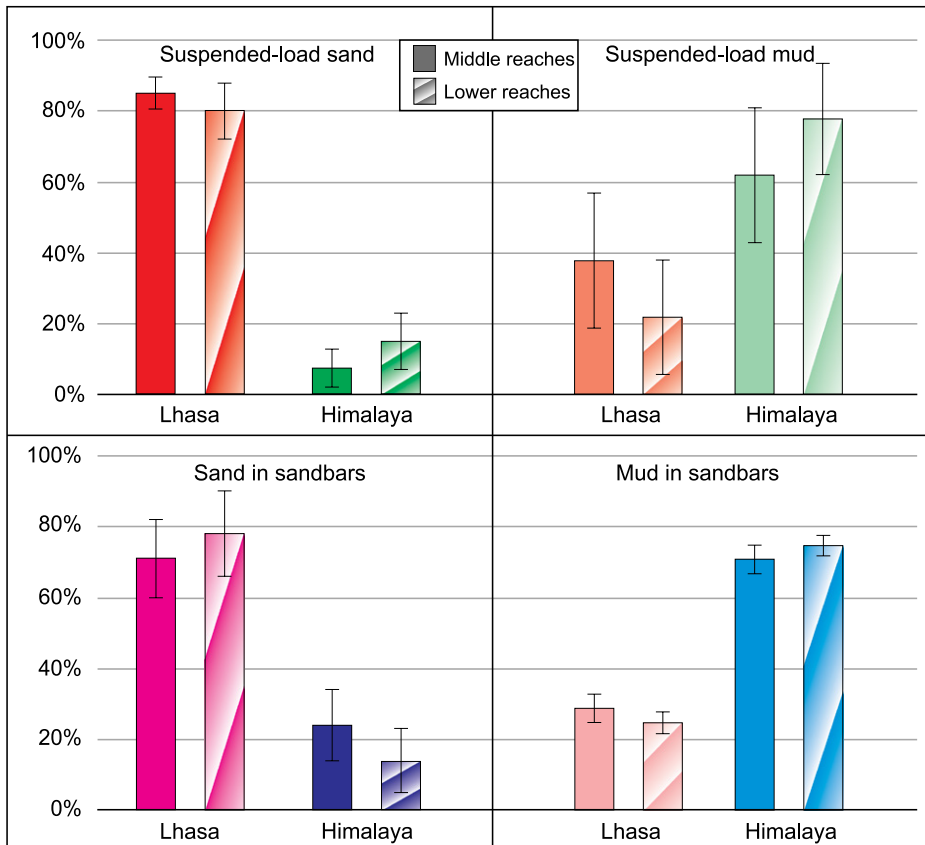


Figure 4. Contrasting provenance budgets from Lhasa block and Himalaya for sand and mud fractions in suspended load and sandbars in Yarlung Tsangpo middle and lower reaches. Error bars indicate ± 1 standard deviation.

and three times more mud than the Lhasa block (Fig. 4). Such a great contrast underscores the fundamental importance of the choice of the grain-size window to be analyzed and calls for the necessity of carefully considering the entire range of grain sizes in quantitative provenance analysis (von Eynatten et al., 2012, 2016; Garzanti et al., 2024).

Sediment Budgets: Suspended Load versus Sandbars

Most sediment in rivers is carried in suspension (e.g., Hay, 1998). It is therefore widely acknowledged that studying suspended load is fundamental to deciphering provenance, erosional, and weathering signals (Viers et al., 2008; Garzanti et al., 2011). Different size fractions of suspended load, however, have been only rarely separated for the accurate assessment of provenance discrepancies.

In our samples, Yarlung Tsangpo suspended load consists of $\sim 79\%$ mud and $\sim 21\%$ sand on average, whereas sandbars consist of $\sim 24\%$ mud and $\sim 76\%$ sand (Fig. S2). The calculated sand and mud contributions (Fig. 4) indicate that the Lhasa block supplies twice as much sediment to sandbars than the Himalayan belt ($\sim 63\%$ versus $\sim 32\%$). In contrast, the Himalayan belt contributes 1.4 times more suspended load than the Lhasa block ($\sim 58\%$ versus $\sim 41\%$).

Such a surprisingly large discrepancy of sediment budgets calculated for suspended load and sandbars is ascribed mainly to grain size–controlled compositional variability, but different transport modes and temporal scales may also be relevant. Sediment can be entrained over long distances in suspension during a single event, i.e., a flood following intense rainfall. Sandbars, instead, invariably consist of a mixture of sediment produced during different episodes and transported in different modes over longer temporal scales ranging from weeks to decades. Different storage times of suspended-load mud and bar sand imply buffering not only of sediment fluxes (Allen, 2008) but also of provenance signals by repeated reworking during river avulsion across the floodplain.

The Yarlung Tsangpo valley includes narrow gorges alternating downstream with wide tracts where large sandbars and dune fields are developed (Wang et al., 2015; Liang et al., 2023). We can thus expect that Himalayan-derived fine-grained sediment carried in suspension is quickly flushed through the system, whereas Lhasa block sand is preferentially stored in the wide parts of the valley and leaves the Tibetan Plateau mainly under strong hydrodynamic conditions (e.g., floods or megafloods).

Revisiting Erosion Patterns: Himalaya versus Lhasa Block

Because of insufficient consideration of suspended load and of its markedly different composition from bedload, all previous studies have indicated the Lhasa block as the dominant sediment source in the Yarlung Tsangpo catchment (Li et al., 2009; Wu et al., 2012; Zhang et al., 2012; Liang et al., 2022; Ma et al., 2023; Du et al., 2024). Contributions from the Himalayan belt have been systematically underestimated in various studies independently of the followed approach—U-Pb age distribution of detrital zircon (Zhang et al., 2012; Ma et al., 2023) and apatite (Du et al., 2024), or petrography and heavy minerals (Liang et al., 2022)—because these studies focused on the sand fraction of fluvial sandbars only. By integrating mud and sand data from both suspended load and bedload and by assuming average bedload to suspended-load ratios between 1:2 and 1:10 for the Yarlung Tsangpo (Pratt-Sitaula et al., 2007), we reckon that the Himalayan belt provides 1.0–1.3 times more sediment than the Lhasa block overall.

Provenance Bias: Sedimentary versus Igneous Sources

Although sediment generation is strongly dependent on weathering regime and tectonic activity, the lithology of parent rocks exerts a primary control on the composition and size distribution of daughter sediment (Johnsson and Basu, 1993). Extreme variations in the sand- versus mud-generation capacity and consequent marked differences between the composition of suspended load and bedload have been documented for specific lithologies such as basalt (Garçon and Chauvel, 2014; Garzanti et al., 2021). The strong contrast between the sediment-generation capacity of sedimentary and felsic igneous rocks is clearly demonstrated in this study, which—conducted under a homogeneous geomorphological and climatic condition—underscores the much greater sand-generation capacity of granitoid rocks in the Lhasa block compared to the much greater mud-generation capacity of sedimentary rocks in the Himalayan belt.

The emblematic case described here has implications for other sedimentary systems worldwide because a heterogeneous geographical distribution of source-rock lithologies is the rule more than the exception in most river catchments. As shown in this Tibetan case, estimates of the relative detrital contribution from sedimentary rocks may be markedly underestimated if provenance budgets are based on the sand fraction only. Correspondingly, the study of finer sediments flushed off river deltas and deposited in distal parts of lakes, seaways, or oceans may lead to overestimation of detrital supply from sedimentary terranes. Because of prominent grain-size effects and different transport modes, the provenance information obtained from all size fractions should be considered jointly to make

accurate geomorphological inferences on the evolution of modern and ancient fluvial systems.

CONCLUSIONS

The Yarlung Tsangpo case indicates a predominant Himalayan contribution for suspended load (~58%) and a predominant Lhasa block contribution for sandbars (~63%). Erosion rate and sediment yield from the Himalayan belt has been systematically and greatly underestimated because previous studies focused on bedload sand only. The great contrast in sand- versus mud-generation potential of sedimentary and granitoid rocks may lead to contrasting sediment budgets based on mud-rich suspended load and sand-rich fluvial bars and, consequently, to large errors in the assessment of sediment budgets and erosion patterns. All components of the sediment flux must be taken into full account to correctly understand geomorphological and paleo-geomorphological processes.

ACKNOWLEDGMENTS

We thank Rob Strachan for careful editorial handling and Devon A. Orme, Laura Stutenbecker, and Jan Schönig for their constructive comments and helpful suggestions. This study was supported financially by the National Natural Science Foundation of China (grant 42202112) and the Second Tibetan Plateau Scientific Expedition and Research Program (STEP, grant 2019QZKK0204).

REFERENCES CITED

Allen, P.A., 2008, From landscapes into geological history: *Nature*, v. 451, p. 274–276, <https://doi.org/10.1038/nature06586>.

Carosi, R., Montomoli, C., Iaccarino, S., and Visonà, D., 2019, Structural evolution, metamorphism and melting in the Greater Himalayan Sequence in central-western Nepal, *in* Treloar, P.J., and Searle, M.P., eds., *Himalayan Tectonics: A Modern Synthesis*: Geological Society, London, Special Publications, v. 483, p. 305–323, <https://doi.org/10.1144/SP483.3>.

Du, Y., Li, G., Liu, D., Wang, X., Cai, D., Dong, X., and Yu, Q., 2024, Application of detrital apatite U-Pb geochronology and trace elements for provenance analysis, insights from a study on the Yarlung River sand: *Journal of Earth Science*, v. 35, p. 1118–1129, <https://doi.org/10.1007/s12583-023-1863-x>.

Garçon, M., and Chauvel, C., 2014, Where is basalt in river sediments, and why does it matter?: *Earth and Planetary Science Letters*, v. 407, p. 61–69, <https://doi.org/10.1016/j.epsl.2014.09.033>.

Garzanti, E., 2019, Petrographic classification of sand and sandstone: *Earth-Science Reviews*, v. 192, p. 545–563, <https://doi.org/10.1016/j.earscirev.2018.12.014>.

Garzanti, E., Andó, S., France-Lanord, C., Censi, P., Vignola, P., Galy, V., and Lupker, M., 2011, Mineralogical and chemical variability of fluvial sediments. 2. Suspended-load silt (Ganga–Brahmaputra, Bangladesh): *Earth and Planetary Science Letters*, v. 302, p. 107–120, <https://doi.org/10.1016/j.epsl.2010.11.043>.

Garzanti, E., Dinis, P., Vezzoli, G., and Borromeo, L., 2021, Sand and mud generation from continental flood basalts in contrasting landscapes and climatic conditions (Paraná–Etendeka conjugate igneous provinces, Uruguay and Namibia): *Sedimentology*, v. 68, p. 3447–3475, <https://doi.org/10.1111/sed.12905>.

Garzanti, E., Bayon, G., Barbarano, M., Resentini, A., Vezzoli, G., Pastore, G., Levacher, M., and

Adeaga, O., 2024, Anatomy of Niger and Benue river sediments from clay to granule: Grain-size dependence and provenance budgets, *Nigeria: Journal of Sedimentary Research*, v. 94, p. 714–735, <https://doi.org/10.2110/jsr.2024.024>.

Hay, W.W., 1998, Detrital sediment fluxes from continents to oceans: *Chemical Geology*, v. 145, p. 287–323, [https://doi.org/10.1016/S0009-2541\(97\)00149-6](https://doi.org/10.1016/S0009-2541(97)00149-6).

Hu, X., Garzanti, E., Moore, T., and Raffi, I., 2015, Direct stratigraphic dating of India-Asia collision onset at the Selandian (middle Paleocene, 59 ± 1 Ma): *Geology*, v. 43, p. 859–862, <https://doi.org/10.1130/G36872.1>.

Ingersoll, R.V., Bullard, T.F., Ford, R.L., Grimm, J.P., Pickle, J.D., and Sares, S.W., 1984, The effect of grain size on detrital modes: A test of the Gazzi-Dickinson point-counting method: *Journal of Sedimentary Research*, v. 54, p. 103–116, <https://doi.org/10.1306/212F83B9-2B24-11D7-8648000102C1865D>.

Jian, X., Zhang, W., Yang, S., and Kao, S., 2020, Climate-dependent sediment composition and transport of mountainous rivers in tectonically stable, subtropical East Asia: *Geophysical Research Letters*, v. 47, <https://doi.org/10.1029/2019GL086150>.

Johnsson, M.J., and Basu, A., eds., 1993, *Processes Controlling the Composition of Clastic Sediments*: Geological Society of America Special Paper 284, 344 p., <https://doi.org/10.1130/SPE284>.

Leeder, M.R., 2011, Tectonic sedimentology: Sediment systems deciphering global to local tectonics: *Sedimentology*, v. 58, p. 2–56, <https://doi.org/10.1111/j.1365-3091.2010.01207.x>.

Li, C., Kang, S., Zhang, Q., and Wang, F., 2009, Rare earth elements in the surface sediments of the Yarlung Tsangbo (Upper Brahmaputra River) sediments, southern Tibetan Plateau: *Quaternary International*, v. 208, p. 151–157, <https://doi.org/10.1016/j.quaint.2009.05.003>.

Liang, W., Garzanti, E., Hu, X., Resentini, A., Vezzoli, G., and Yao, W., 2022, Tracing erosion patterns in South Tibet: Balancing sediment supply to the Yarlung Tsangpo from the Himalaya versus Lhasa Block: *Basin Research*, v. 34, p. 411–439, <https://doi.org/10.1111/bre.12625>.

Liang, W., Hu, X., Garzanti, E., Dong, X., and Zhang, Y., 2023, Fluvial-aeolian interaction and compositional variability in the river-fed Yarlung Tsangpo dune system (southern Tibet): *Journal of Geophysical Research: Earth Surface*, v. 128, <https://doi.org/10.1029/2022JF006920>.

Liedel, S., Caracciolo, L., Beltrán-Triviño, A., Restrepo, J.C., Restrepo Ángel, J.D., and Sczerba, M., 2024, A quantitative provenance analysis (QPA) approach to quantify controls on sediment generation and sediment flux in the upper reaches of the Magdalena River (Colombia): 2. Lithological control on contribution to silt- to clay-sized fractions: *Journal of Geophysical Research: Earth Surface*, v. 129, <https://doi.org/10.1029/2023JF007379>.

Ma, X., Li, S., and Yue, Y., 2023, Provenance analysis of wind-formed dunes in the Shannan broad valley of the Yarlung-Zangbu River based on detrital zircon characteristics: *Quaternary Sciences (Disiji Yanjiu)*, v. 43, p. 1157–1171 [in Chinese with English abstract].

Pan, G., Ding, J., Yao, D., and Wang, L., 2004, Geological map of Qinghai-Xizang (Tibet) Plateau and adjacent areas: Chengdu, Chengdu Cartographic Publishing House, scale 1:1,500,000.

Peng, S., 2024, 1 km monthly precipitation dataset over China during 1901–2023 [Dataset]: National Earth System Science Data Center, National Science & Technology Infrastructure of China, <https://doi.org/10.12041/geodata.192891852410344.ver1.db>.

Pratt-Sitaula, B.A., Garde, M., Burbank, D.W., Oskin, M.E., Heimsath, A.M., and Gabet, E.J., 2007, Bedload-to-suspended load ratio and rapid bedrock incision from Himalayan landslide-dam lake record: *Quaternary Research*, v. 68, p. 111–120, <https://doi.org/10.1016/j.yqres.2007.03.005>.

Resentini, A., Goren, L., Castellort, S., and Garzanti, E., 2017, Partitioning the sediment flux by provenance and tracing erosion patterns in Taiwan: *Journal of Geophysical Research: Earth Surface*, v. 122, p. 1430–1454, <https://doi.org/10.1002/2016JF004026>.

Sciunnach, D., and Garzanti, E., 2012, Subsidence history of the Tethys Himalaya: *Earth-Science Reviews*, v. 111, p. 179–198, <https://doi.org/10.1016/j.earscirev.2011.11.007>.

Singh, S.K., and France-Lanord, C., 2002, Tracing the distribution of erosion in the Brahmaputra watershed from isotopic compositions of stream sediments: *Earth and Planetary Science Letters*, v. 202, p. 645–662, [https://doi.org/10.1016/S0012-821X\(02\)00822-1](https://doi.org/10.1016/S0012-821X(02)00822-1).

Stutenbecker, L., Scheuven, D., Hinderer, M., Hornung, J., Petschick, R., Raila, N., and Schwind, E., 2023, Temporal variability of fluvial sand composition: An annual time series from four rivers in SW Germany: *Journal of Geophysical Research: Earth Surface*, v. 128, <https://doi.org/10.1029/2023JF007138>.

Viers, J., Roddaz, M., Filizola, N., Guyot, J.-L., Sondag, F., Brunet, P., Zouiten, C., Boucayrand, C., Martin, F., and Boaventura, G.R., 2008, Seasonal and provenance controls on Nd–Sr isotopic compositions of Amazon rivers suspended sediments and implications for Nd and Sr fluxes exported to the Atlantic Ocean: *Earth and Planetary Science Letters*, v. 274, p. 511–523, <https://doi.org/10.1016/j.epsl.2008.08.011>.

von Eynatten, H., Tolosana-Delgado, R., and Karius, V., 2012, Sediment generation in modern glacial settings: Grain-size and source-rock control on sediment composition: *Sedimentary Geology*, v. 280, p. 80–92, <https://doi.org/10.1016/j.sedgeo.2012.03.008>.

von Eynatten, H., Tolosana-Delgado, R., Karius, V., Bachmann, K., and Caracciolo, L., 2016, Sediment generation in humid Mediterranean setting: Grain-size and source-rock control on sediment geochemistry and mineralogy (Sila Massif, Calabria): *Sedimentary Geology*, v. 336, p. 68–80, <https://doi.org/10.1016/j.sedgeo.2015.10.008>.

Wang, Z., Yu, G., Wang, X., Melching, C.S., and Liu, L., 2015, Sediment storage and morphology of the Yalu Tsangpo valley due to uneven uplift of the Himalaya: *Science China Earth Sciences*, v. 58, p. 1440–1445, <https://doi.org/10.1007/s11430-015-5113-7>.

Wu, W., Zheng, H., Xu, S., Yang, J., and Yin, H., 2012, Geochemistry and provenance of bed sediments of the large rivers in the Tibetan Plateau and Himalayan region: *International Journal of Earth Sciences*, v. 101, p. 1357–1370, <https://doi.org/10.1007/s00531-011-0719-2>.

Zhang, J., Yin, A., Liu, W., Wu, F., Lin, D., and Grove, M., 2012, Coupled U–Pb dating and Hf isotopic analysis of detrital zircon of modern river sand from the Yalu River (Yarlung Tsangpo) drainage system in southern Tibet: Constraints on the transport processes and evolution of Himalayan rivers: *Geological Society of America Bulletin*, v. 124, p. 1449–1473, <https://doi.org/10.1130/B30592.1>.

Zhu, D., Zhao, Z., Niu, Y., Mo, X., Chung, S., Hou, Z., Wang, L., and Wu, F., 2011, The Lhasa Terrane: Record of a microcontinent and its histories of drift and growth: *Earth and Planetary Science Letters*, v. 301, p. 241–255, <https://doi.org/10.1016/j.epsl.2010.11.005>.

Printed in the USA